USA-JAPAN WORKSHOP

ON SUBMILLIMETER DIAGNOSTIC TECHNIQUES

January 18-21, 1982

Nagoya, Japan

MULTI-MIXER FAR-INFRARED SCATTERING APPARATUS

H.K. Park, C.X. Yu, R. Savage, W.A. Peebles and N.C. Luhmann, Jr.

University of California

Los Angeles, California

A multi-mixer far-infrared scattering system has been developed which permits the collection of angularly and spatially resolved collective scattering data during a single tokamak discharge.

1. INTRODUCTION

Recent improvements in far-infrared CW source and detector technology have made it possible to perform collective scattering studies from waves in both laboratory and fusion plasmas. Specifically, CW scattering has been successfully performed from driven ion acoustic waves in an unmagnetized filament discharge plasma[1], density perturbations associated with resonance absorption of electromagnetic radiation in an unmagnetized inhomogeneous plasma[2], spontaneously occurring low frequency microturbulence in a tokamak plasma[3] and more recently from mode converted ion Bernstein waves associated with tokamak ICRF heating.[4] Unfortunately, because only a single detector channel was available, wave dispersion relations were obtained in these studies by a shot-to-shot variation of the scattering collection angles. Therefore, the reliability of the frequency and wavenumber spectra were totally dependent upon the reproducibility of the plasma and the phenomena under investigation. In the study of random processes such as low frequency microturbulence the fact that there is only a single channel is an obvious restriction. In addition, diagnostic applications such as ion temperature determination via CW scattering from externally launched waves are dependent upon single-shot time resolved wave dispersion data.

To satisfy the abovementioned needs, a multi-mixer far-infrared scattering apparatus has been developed at UCLA. In this system, the FIR radiation scattered from plasma density fluctuations is collected by six mirrors which are designed to accept signals corresponding to six discrete wavenumbers. In the case of a 1.22 mm wavelength probe beam this corresponds to obtaining spectral information in the 0-20 cm^{-1} region. The scattered radiation in each channel is combined with a local oscillator signal and downconverted in a

quasi-optical biconical Schottky barrier diode mixer.[5] Separate low noise (≃ 1.5 - 2 dB) IF amplifier systems (≃ 60 - 90 dB gain) are employed to amplify the frequency downconverted signals to a level sufficiently high for subsequent data processing. In order to accurately obtain dispersion relations as well as the absolute level of the density fluctuations, considerable effort has been devoted to the system calibration. To achieve this goal, system parameters such as collection efficiency, wavenumber resolution, scattering volume and detector sensitivities have been carefully measured. The calibration procedures have included acoustic cells[6], laboratory test wave scattering as well as standard hot-cold load techniques.

This paper contains a description of the first multi-mixer FIR scattering system which permits the acquisition of spatially and temporally resolved single shot dispersion data. The organization of the paper is as follows. In Sec. 2, the design of the scattering apparatus is discussed in detail. The calibration procedures including the design of the acoustic cell are presented in Sec. 3.

2. MULTI-MIXER SCATTERING APPARATUS

The design of the multi-mixer scattering apparatus depicted schematically in Fig. 1 is based on our previous experience in laboratory[1,2] and tokamak[3,4] FIR scattering studies. All of the optical components are mounted on a 120 x 160 cm aluminum tool plate using sets of precision dowel pins and holes. There are no adjustments except for the quasi-optical mixers which are mounted on optical translation stages. The mirrors are machined out of solid aluminum and are polished sufficiently well to permit system alignment with a visible laser which ensures low loss in the far-infrared. The mirrors have been wedge cut so that each channel subtends the same solid angle.

As shown in Fig. 1, the homodyne system employs a large number of beamsplitters (of varying transmission) to separate the probe beam and local oscillator beams as well as to combine the scattered beams and LO beams prior to focussing them into the mixers. The beamsplitters are made of electroformed nickel meshes stretched across cylindrical aluminum support rings with a 45° cut to minimize beam interception. Various mesh constants ($\simeq$ 75 - 250 lines per cm) are employed to optimize reflectivities such that equal amounts of local oscillator power are provided to each channel.

Thus far, all of the measurements have been performed using an optically pumped FIR laser operating at $\lambda_o \simeq 1.22$ mm as the probe source. The design is similar to that described in Refs. 7 and 8, except that it has been optimized for operation at this wavelength and provides $\simeq$ 7 - 10 mW of output power. In this case, 80% of the FIR output is reflected by the first beamsplitter ($\simeq$ 40 lines per cm) shown in Fig. 1 and then divided equally using a set of beamsplitters with varying mesh constants. The probe beam is focussed onto the plasma center via a long focal length (f.l. $\simeq$ 100 cm) polyethylene lens. The scattered beams

and LO beams are combined in 50% beamsplitters and focussed into the quasi-optical biconical mixers using f/0.5 polyethylene lenses.

For the case of a normally incident probe beam the collection angles range from 0 - 22.5° as shown in Fig. 1. By changing the angle of incidence of the beam to either 1.5° or 3°, the corresponding range of collection angles is 1.5 - 24° and 3 - 25.5°, respectively. Here it should be noted that the 0° channel can be employed for interferometry measurements.

In addition to the possibility of simultaneous angular scattering measurements, the system may be configured to provide a simultaneous multi-spatial position scattering capability. Such a system is extremely useful for studies such as the recent mode converted ion Bernstein wave measurements on the UCLA Microtor tokamak.[4] The configuration illustrated schematically in Fig. 2 provides the capability of simultaneously observing the time history of the waves at three different spatial locations. The three beamsplitters shown in Fig. 2 result in probe beams at three different spatial positions. The scattered beams are collected by rotatable collection mirrors mounted on translation stages.

3. SCATTERING SYSTEM CALIBRATION

As mentioned earlier, it is necessary to precisely measure scattering parameters such as scattering length and wavenumber resolution in order to obtain accurate wave dispersion relations and amplitudes via collective scattering. Specifically, absolute density fluctuation and spectral density ($S(\hat{k})$) measurements require an absolute calibration of the entire optical system as well as the receiver system.

An acoustic cell similar to that utilized by the Kyoto University group[6] is employed for optical system calibration. As shown in Fig. 3, the acoustic cell consists of a main body possessing good transmission at the desired FIR operating frequency (e.g. polyethylene) and a piezoelectric transducer (PZT) to launch acoustic waves of the appropriate frequency. Unfortunately, even if the PZT driving voltage is kept constant the amplitude of the acoustic waves is a sensitive function of frequency. This variation arises since PZT transducers exhibit a series of resonances related to their thickness d by

$$d = \frac{\lambda}{2}, \frac{3\lambda}{2}, \frac{5\lambda}{2}, \quad \ldots\ldots$$

where λ is the acoustic wavelength in the PZT transducer. Because of this strong frequency dependence, the amplitude of launched waves must be measured within the acoustic cell at each frequency. As shown in Fig. 3, this is accomplished by means of small angle He-Ne laser scattering orthogonal to the FIR scattering plane. To accomplish this, TPX plastic (5 x 5 x 15 cm) is employed as the main body since it has good transmission in the FIR as well as adequate transmission in the visible. A 1.5 mW CW HeNe laser is employed as the probe source with detection accomplished using a photomultiplier tube. The resultant frequency responses are shown in Fig. 4 for two different PZT thicknesses (d = 1.27 cm, 2.2 cm) with the ac excitation voltage held constant at ≈ 50 V. The resonances

are obvious. To provide flexibility in system calibration we therefore do not permanently attach the transducers to the cell bodies but instead simply clamp them solidly to the body with a small amount of vacuum grease at the interface. This technique provides good acoustic coupling and yet facilitates the selection of varying PZT thicknesses for frequency selection.

The accuracy of the system calibration is obviously dependent on a precise knowledge of the acoustic wavelength within the cell. As shown in Fig. 5, this measurement is easily performed using a time of flight technique to determine the sound speed in the medium (and thus k since ω is known). Here, the PZT excitation voltage is no longer a steady sinusoid, but is instead gated using a tone burst generator. From the measurements shown in Fig. 5 we see that the sound speed in TPX is $\approx 2.2 \times 10^5$ cm/sec. Here it should be noted that this time of flight technique was greatly facilitated by cutting the "sawtooth" pattern on the end of the cell body (see Fig. 3) to eliminate reflections and possible resonance problems. Basically, this simply serves as a "beam dump." As a final point it should be noted that the acoustic cell displays the same behavior as a classical damped oscillator when driven on or off-resonance. This is clearly illustrated in Fig. 6.

Despite their convenience, acoustic cells do have some associated problems which must be noted. First, there is obviously a bending of the FIR radiation at the dielectric-air interface for all angles other than exact normal incidence. One must therefore employ Snell's law and correct the data for this angular shift. A second difficulty is associated with the PZT resonances described earlier. As we shall see in the following, the fourth scattering channel ($\theta_s = 13.5^o$) has not yet been calibrated due to a lack of acoustic cell response at the appropriate frequencies.

Using the above described techniques we then proceeded to calibrate the optical system. First, the wavenumber resolution for each channel was determined.

In this measurement, the acoustic frequency (and hence wavenumber) was varied while the acoustic wave amplitude was held constant (monitored by He-Ne laser scattering) and the scattered power monitored on the appropriate channel. The result is a plot for each channel as shown in Fig. 7. From these curves we find that the wavenumber resolution $\Delta k \simeq 1.1$ cm^{-1} measured at the electric field e^{-1} points. This result is in good agreement with the theoretically predicted value $\Delta k \simeq 2/a_o$ using the separately measured value $a_o \simeq 1.8$ cm for the beam waist.

The scattering length was determined by scanning the acoustic cell along the incident beam and monitoring the scattered power. The experimental results are shown in Fig. 8. The scattering length defined as the full-width at half maximum of these curves is in good agreement with the theoretical value $\ell_v = 2a_o/\sin\theta_s$. Here it should be noted that for the 4.5° and 9° channels the scattering lengths are longer than the diameter of the Microtor tokamak plasma ($2a \simeq 20$ cm).

The final optical system parameter that must be obtained is the relative collection efficiency of the various channels. This is determined by measuring the signal level on each channel for a fixed acoustic wave amplitude where the appropriate acoustic wavelength is selected for each channel. The results are shown in Fig. 9.

In addition to the optical system, the mixer and IF systems must also be calibrated. This is accomplished using standard hot-cold load techniques and Y-factor analysis. The load material utilized for the FIR measurements is Eccosorb (manufactured by Emerson-Cumming) with the hot load at room temperature and the cold load cooled to 77°k (LN_2 temperature). Double sideband system noise temperatures of $\simeq$ 5000 - 10,000°k are obtained in this system.

4. SUMMARY

In summary, a multi-mixer FIR scattering system has been developed which permits the collection of angular and spatial resolved scattering data on a single shot. Calibration procedures have been developed and successfully implemented. More recently, the system has been installed on the UCLA Microtor tokamak and will be utilized in the ICRF measurements.

Acknowledgements

The work was supported by the U.S. Department of Energy, Office of Fusion Energy under Contract No. DE-AM03-76SF00010.

References

1. H. Park, W.A. Peebles, A. Mase, N.C. Luhmann, Jr. and A. Semet, Appl. Phys. Lett. 37, 279 (1980).
2. C.X. Yu, H. Park, W.A. Peebles and N.C. Luhmann, Jr., to be published.
3. A. Semet, A. Mase, W.A. Peebles, N.C. Luhmann, Jr. and S. Zweben, Phys. Rev. Lett. 45, 445 (1980).
4. P. Lee, R.J. Taylor, W.A. Peebles, H. Park, C.X. Yu, Y. Xu, N.C. Luhmann, Jr. and S.X. Jin, UCLA PPG-577, submitted to Phys. Rev. Lett.
5. J.J. Gustincic, Proc. of Soc. of Photo-Optical Instr. Engrs. 105, 40 (1977).
6. T. Saito, M. Ikeda, Y. Hamada, T. Yamashita, M. Nakamura and S. Tanaka, Proc. of Int. Conf. on Plasma Physics, Joint Conf. of 4th Kiev Int. Conf. on Plasma Theory and 4th Int. Congress on Waves and Instabilities Vol. I, 349 (1980).

OPTICAL SYSTEM FOR MULTI-MIXER SCATTERING

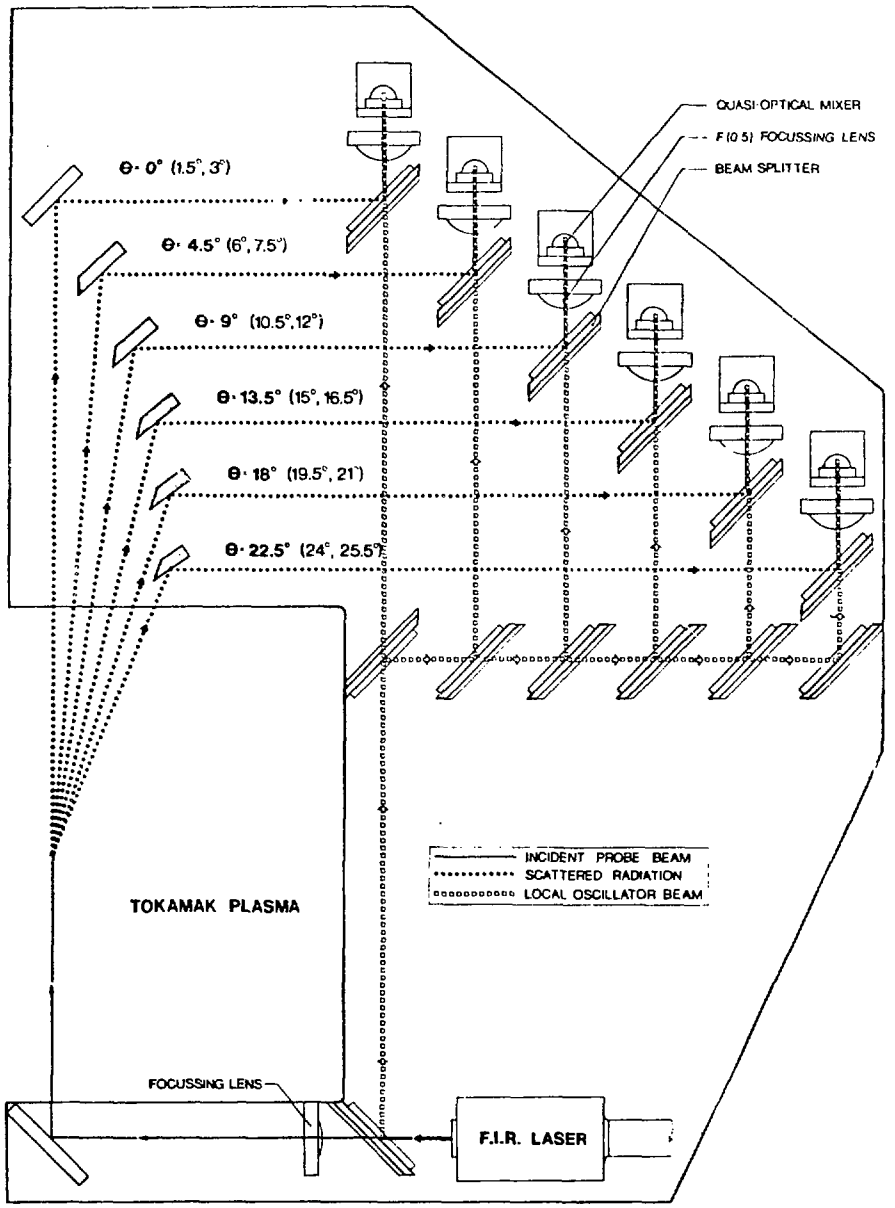

Fig. 1 Experimental arrangement of FIR scattering system for single shot wave dispersion determination.

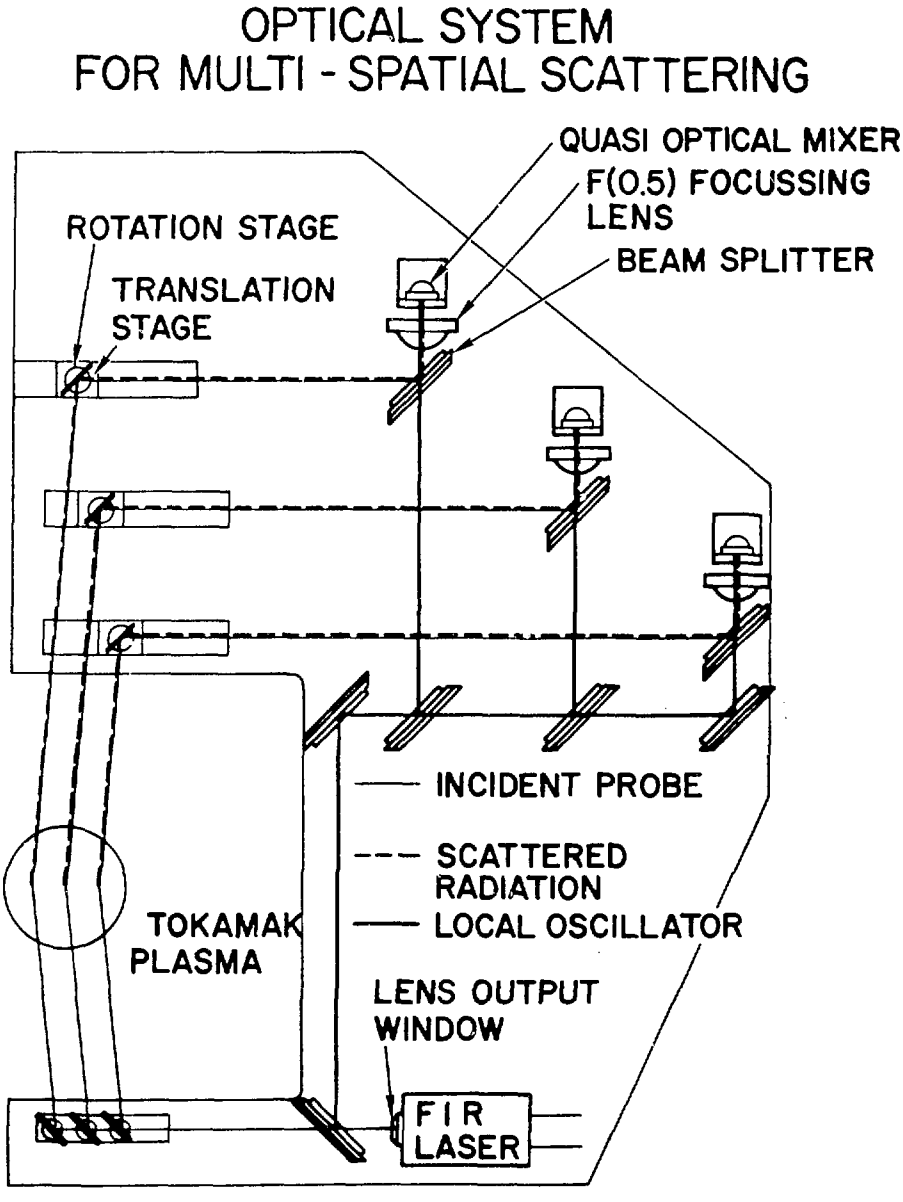

Fig. 2 Experimental arrangement of FIR multi-spatial scattering system.

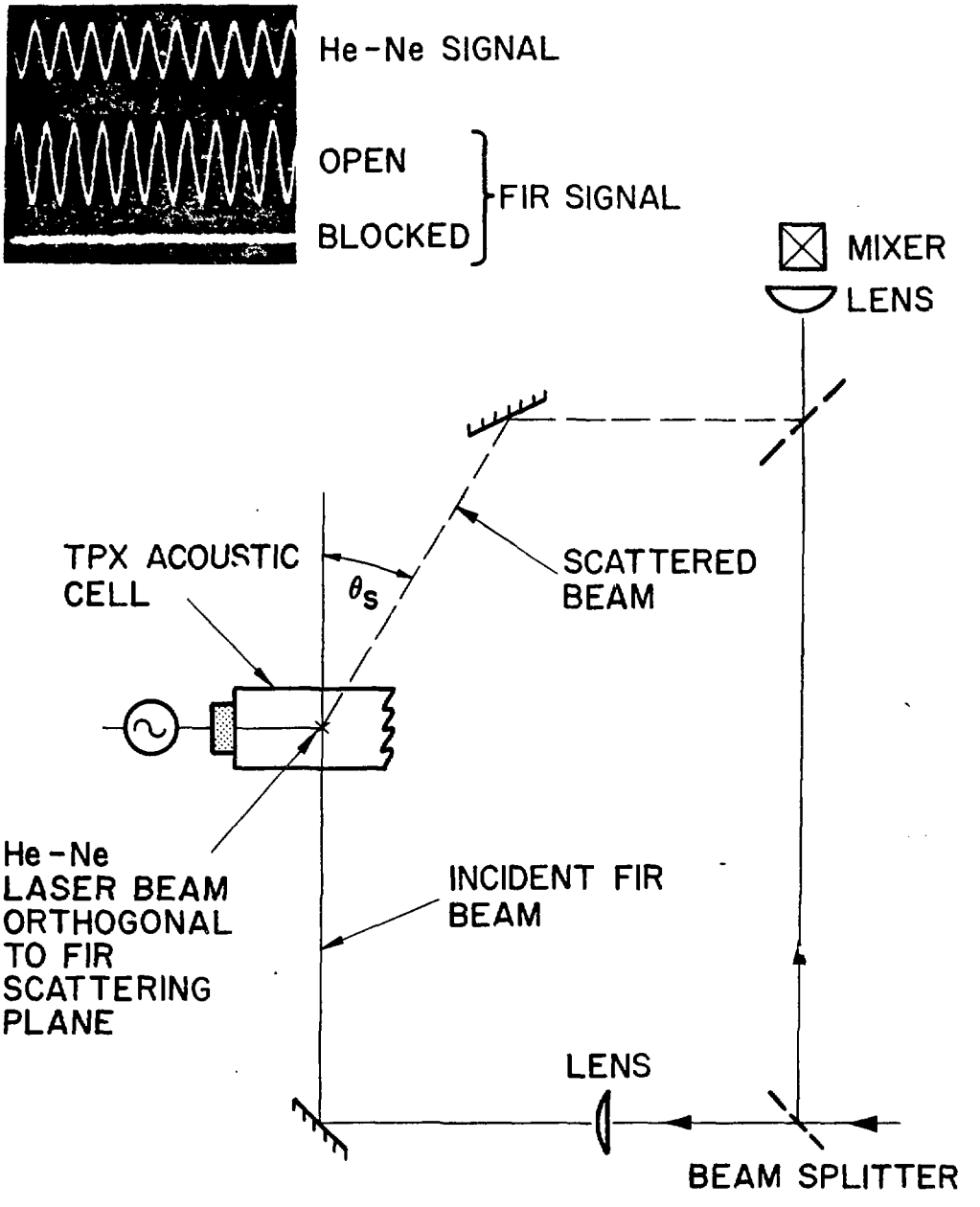

Fig. 3 Experimental arrangement for TPX acoustic cell calibration of optical system.

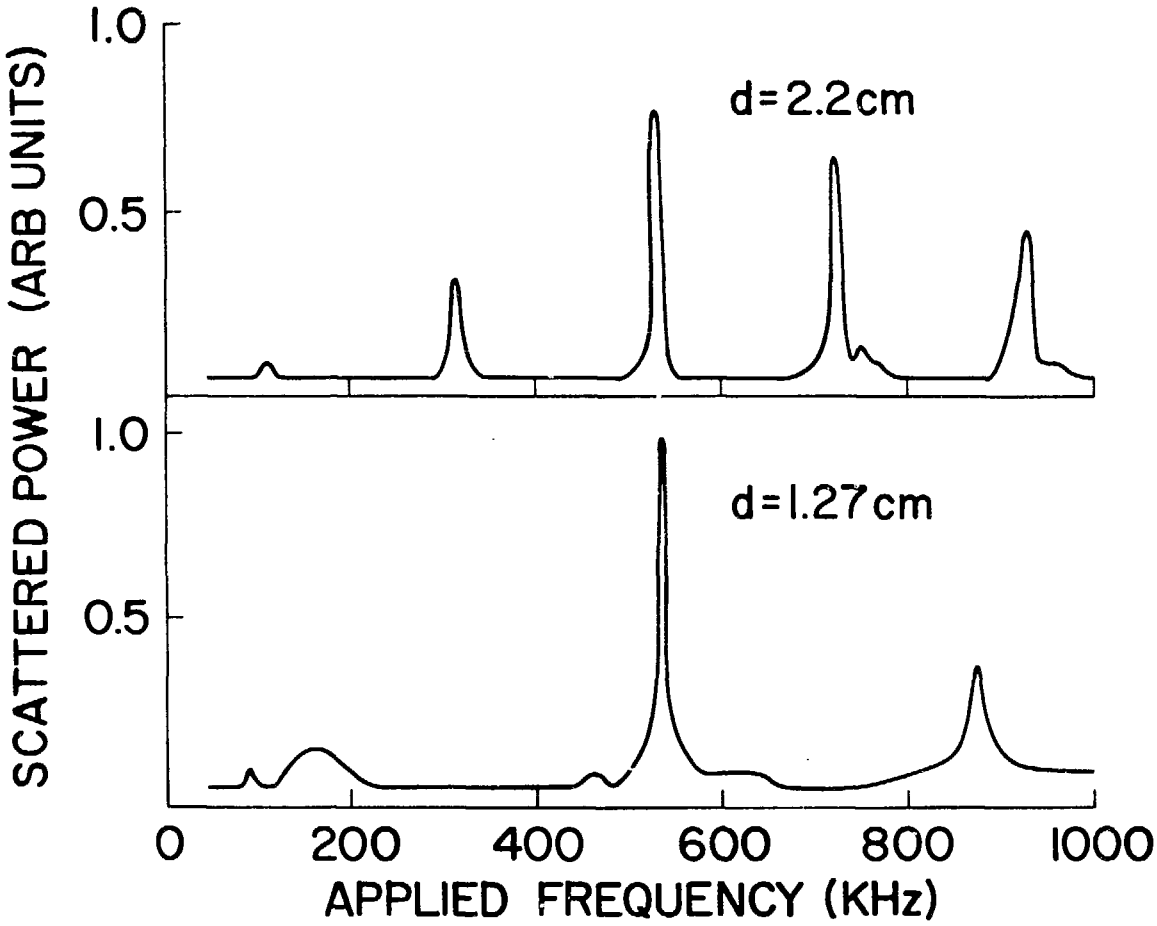

Fig. 4 Acoustic cell frequency response with two different thickness piezoelectric transducers.

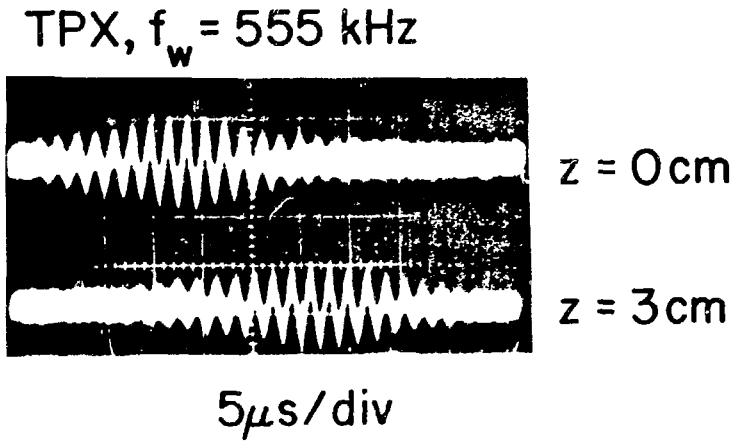

Fig. 5 Time of flight determination of acoustic speed (and hence wavenumber) in TPX acoustic cell.

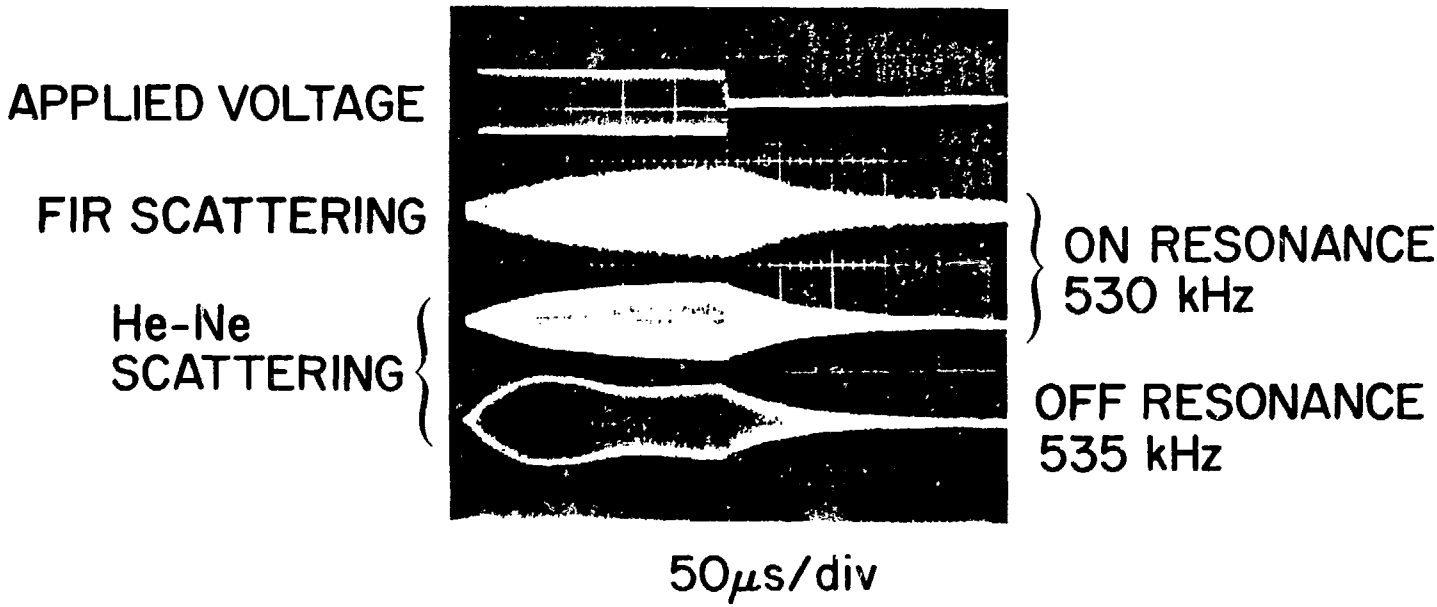

Fig. 6 FIR and He-Ne scattering response from acoustic cell driven on- and off-resonance with a tone burst generator.

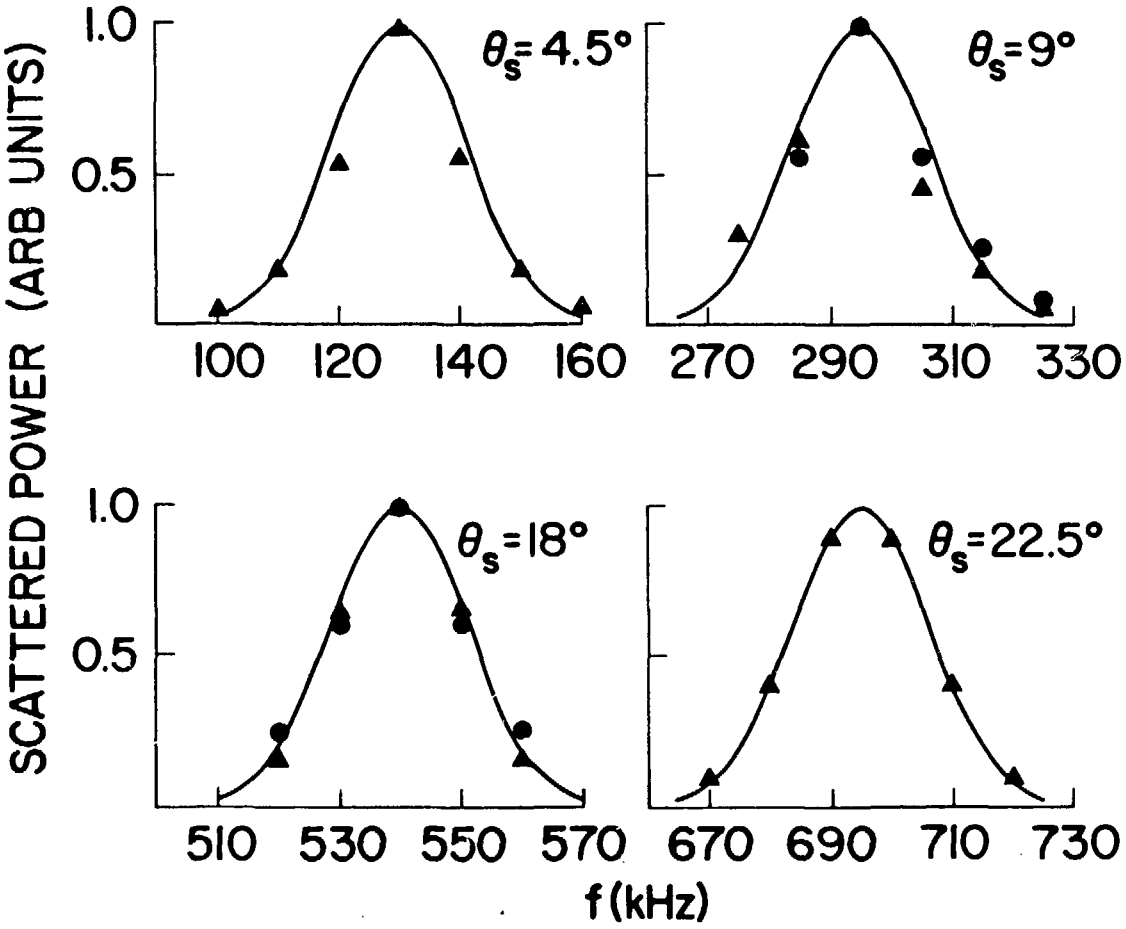

Fig. 7 Acoustic cell calibration of scattering system wavenumber resolution.

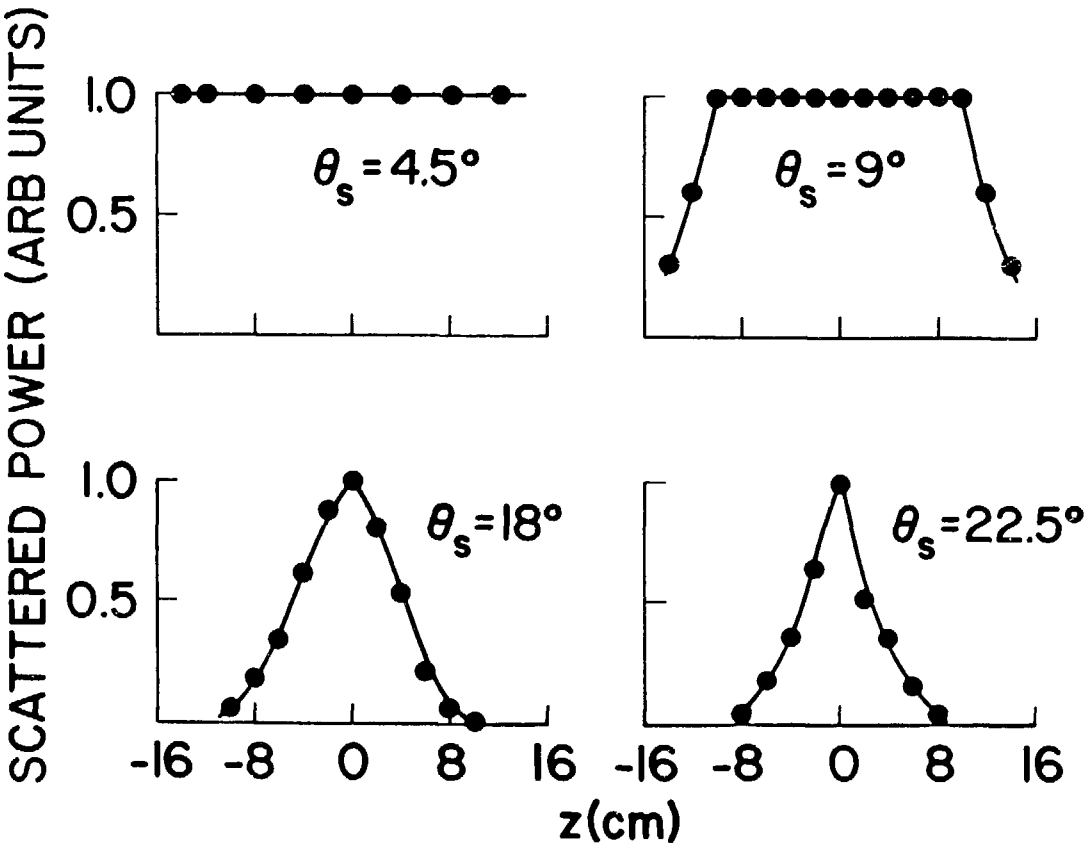

Fig. 8 Acoustic cell calibration of scattering length for four of the system channels.

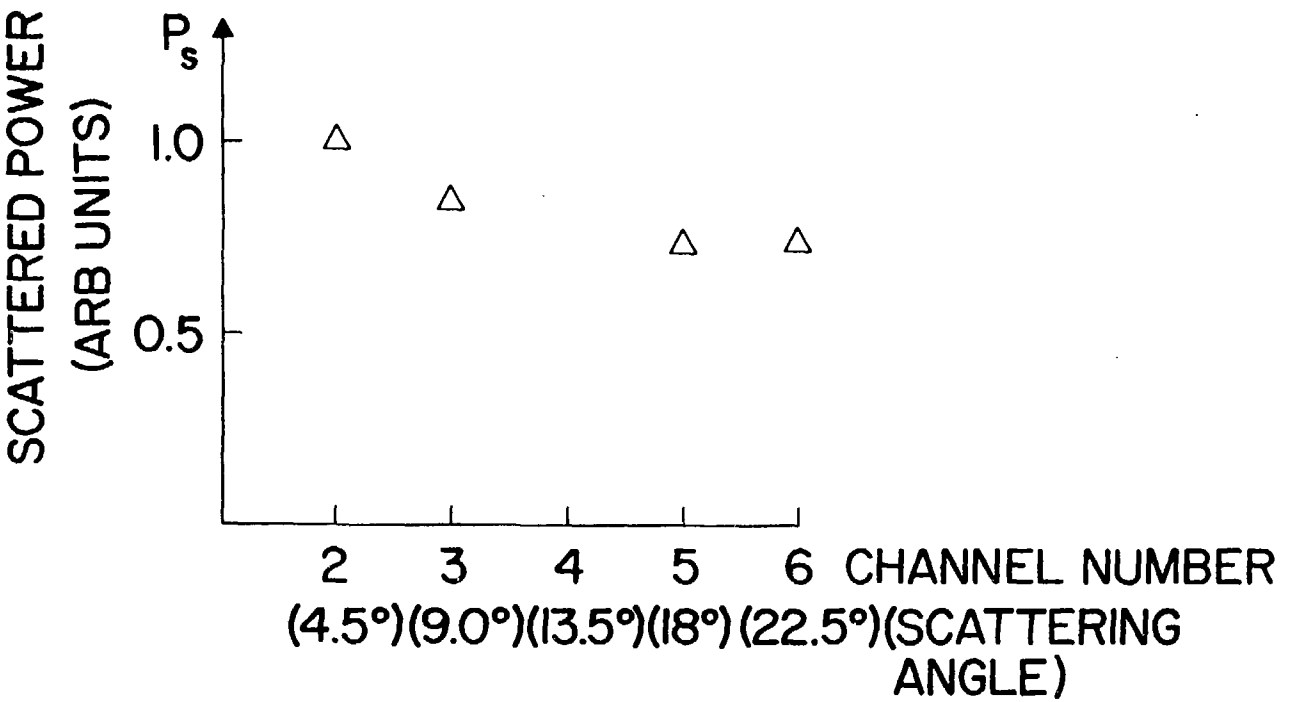

Fig. 9 Acoustic cell calibration of collection efficiency for four of the system channels.